Detection of high-altitude ionospheric irregularities with GPS/MET

Sergey Sokolovskiy,[1] William Schreiner, Christian Rocken, and Douglas Hunt
GPS Science and Technology Program, University Corporation for Atmospheric Research, Boulder, Colorado USA

Received 7 May 2001; revised 2 January 2002; accepted 3 January 2002; published 14 February 2002.

[1] In this study radio occultation data from the GPS/MET experiment are used for detection of high-altitude ionospheric irregularities. This is done by back propagation of the complex electromagnetic field observed in orbit while accounting for the direction of the Earth's magnetic field. The irregularities are detected mainly in the F region. However, for some occultations they are detected above the F2 peak at altitudes up to 1000 km and higher. Results of numerical simulations, a description of the used algorithm, and examples of the processed GPS/MET data are presented. *INDEX TERMS:* 2439 Ionosphere: Ionospheric irregularities; 2487 Ionosphere: Wave propagation (6934); 2494 Ionosphere: Instruments and techniques; 2415 Ionosphere: Equatorial ionosphere

1. Introduction

[2] Detection, localization, and estimation of the structure of irregularities of electron density in the ionosphere have been done in a number of studies by use of radio holographic (RH) methods applied to ground received satellite signals [*Schmidt and Tauriainen*, 1975; *Kunitsyn*, 1986; *Tereshchenko*, 1998]. Recently radio occultation (RO) data have been used for monitoring Earth's neutral atmosphere [*Kursinski et al.*, 1997; *Rocken et al.*, 1997] and ionosphere [*Hajj and Romans*, 1998; *Schreiner et al.*, 1999]. The refractivity, retrieved under the assumption of the local spherical symmetry, is assigned to the tangent point (TP) of the line of sight (LS) from GPS to low Earth orbiter (LEO). In a few studies GPS/MET RO data have been used for localization of refractivity irregularities in the ionosphere. *Vorob'ev et al.* [1999] and *Sokolovskiy* [2000] suggested and tested a simple approach, introducing the refractivity irregularities by an equivalent phase screen (PS). The position of the PS along the LS was estimated based on agreement of the bending angles calculated from phase and amplitude separately. *Gorbunov et al.* [2002] apply back propagation of the complex electromagnetic (EM) field recorded by LEO and localize refractivity irregularities in the E layer by analyzing the amplitude of the 2-D EM field. *Hocke and Tsuda* [2001] analyzed the statistics of irregularities in the E layer by associating them with the small-scale fluctuation in TEC along the LS at TP altitudes typical for the E layer.

[3] Commonly the amplitude of RO signals does not undergo strong scintillation at TP altitudes above the neutral atmosphere and below the E layer of the ionosphere. However, for some occultations amplitude scintillation is large at all TP altitudes. Figure 1A shows an example of the typical RO L1 signal, while Figures 1B and 1C show the examples affected by large scintillation. Obviously, the refractivity irregularities causing this scintillation are not located at the TP of the LS.

[4] Since EM signals are received along a 1-D trajectory, an assumption about the structure of the refractivity is needed to reduce the dimension of the inverse problem. A common approach, applied in RO data processing, is to reduce the inverse problem to 2-D in the vertical plane by assuming that the EM field does not vary in the transverse direction. This approximation is feasible for the neutral atmosphere and for the E layer of the ionosphere where the refractivity irregularities can approximately be treated as horizontally homogeneous. However, at higher altitudes, in the F layer and above, where the irregularities are commonly elongated along the direction of magnetic field, accounting for their structure is necessary to minimize errors of their localization.

[5] In this study we first performed numerical simulations of the 2-D and 3-D forward propagation (FP) and back propagation (BP) of EM waves for isotropic and anisotropic refractivity irregularities, introducing them by an equivalent PS. Next, we have developed an algorithm of the 2-D BP of RO signals that accounts for the model of the Earth's magnetic field. The algorithm has been tested by using 50 Hz GPS/MET RO data. Since a typical transversal velocity of the LS is 2–3 km/sec, the use of high rate data allows sub-Fresnel resolution of the received EM signal. A number of cases have been found where the ionospheric irregularities were localized at high altitudes, in the F layer and above.

2. Use of Back Propagation for Localization of Refractivity Irregularities

[6] For the simulations we introduce the refractivity irregularities by a plane phase screen. We solve the 2-D and 3-D scalar FP and BP problems (Helmholtz equation in a vacuum) by expanding the complex EM field $u = a\exp(iks)$ ($k = 2\pi f/c$, c is light velocity in vacuum, $f = 1.57542$ GHz for L1 GPS signal) in a series of plane waves. This technique is commonly used, it can be found in [*Martin*, 1993]. We assume an incident plane wave propagating along the X direction. The results of the simulations are summarized in Figure 2.

[7] The effect of anisotropic refractivity irregularities is modeled by a random 1-D PS in the Y, Z plane at $x = 0$, as shown in Figure 2A. Figure 2A0 shows the amplitude a of the EM field in the X, Y plane after FP through the screen. As seen, focusing/defocusing results in increase of the amplitude modulation with increasing x. Figure 2A1 shows the amplitude of the EM field after BP by using u at $x = 3000$ km as the boundary condition. At $x > 0$ the BP EM field agrees with the FP EM field, while at $x < 0$ amplitude modulation increases due to the imaginary focusing/defocusing. Thus the position of the PS can be estimated by finding the minimum of the amplitude modulation of the 2-D BP EM field.

[8] Next, we assumed that the complex signal u is observed at $x = 3000$ km along the trajectory inclined by angle $\alpha = 15°$ with respect to X, Y plane, as shown by line in Figure 2A. No additional FP is necessary because the EM field does not depend on z and thus recording a signal along the inclined trajectory is equivalent to its elongation with the factor $1/\cos\alpha$. The result of the 2-D BP with the use of such elongated signal at $x = 3000$ km as the boundary condition is shown in Figure 2A2. As seen, the amplitude of the BP EM field again has a clear minimum of modulation, but that minimum is shifted by about 250 km.

[9] Next, we modeled the effect of an extended volume filled with irregularities by using 10 random uncorrelated 1-D phase

[1] Also at A. M. Obukhov Institute of Atmospheric Physics, Moscow, Russia.

Copyright 2002 by the American Geophysical Union.
0094-8276/02/2001GL013398$05.00

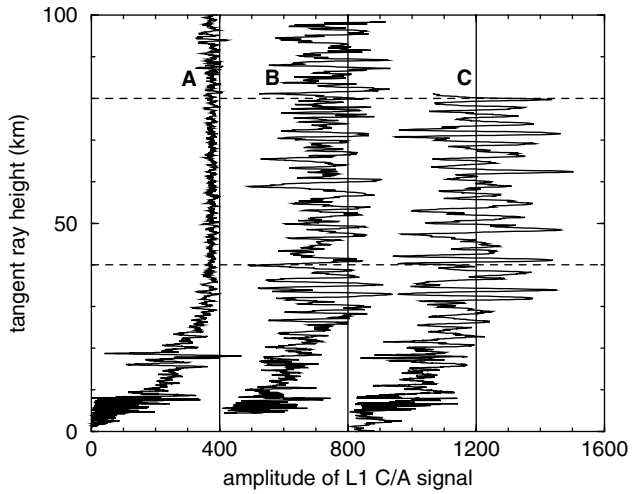

Figure 1. Examples of RO amplitude (in conventional units) for three GPS/MET occultations. B and C are shifted by 400 and 800 units for display purposes.

screens evenly spaced along X between −500 km and +500 km. Figure 2A3 shows the BP amplitude in XY plane (the FP amplitude is not shown). As seen, the position of the volume (outlined by two dashed lines) still can be fairly well detected based on the minimum of BP amplitude modulation.

[10] Finally, we modeled the effect of isotropic refractivity irregularities by a random 2-D PS in the Y, Z plane at $x = 0$, as shown in Figure 2B. Figure 2B0 shows X, Y cross section of the 3-D FP EM field whose structure looks similar to that in Figure 2A0. 3-D BP, performed for validation purposes (not shown), results in a clear minimum of the amplitude modulation at $x = 0$, similarly to that shown in Figure 2A1. However, if 2-D BP is applied in any plane, i.e., by using u obtained in any cross section at $x = 3000$ km as the boundary condition, then the BP EM field does not show evidence of a minimum of amplitude modulation at any distance. This is shown in Figure 2B1.

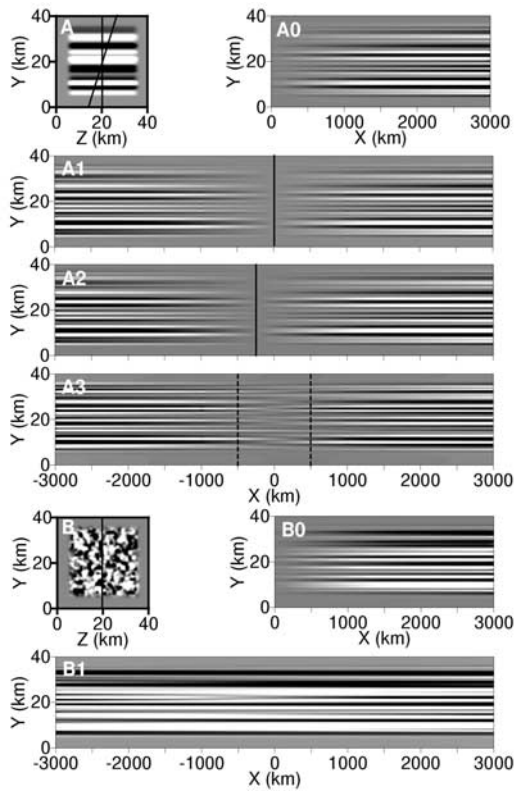

Figure 2. Results of the numerical simulations of the 2-D and 3-D forward and back propagation.

[11] As it follows from the simulations, the localization of irregularities by 2-D BP is possible for anisotropic (elongated) irregularities with the orientation of the BP plane transverse to the irregularities. Since in the F layer and above the irregularities of electron density are commonly elongated along magnetic field, we developed an algorithm for their localization which uses the model of the Earth's magnetic field [*Barton*, 1997].

[12] In RO the complex EM field is recorded along a curved LEO trajectory rather than a straight line. In this case we use the the following approximate solution of the 2-D BP problem [*Baker and Copson*, 1987; *Gorbunov et al.*, 2002]

$$u(\mathbf{r}) = \sqrt{\frac{k}{2\pi}} \int u(\mathbf{r}') \cos\varphi \frac{\exp(-ik|\mathbf{r}-\mathbf{r}'| + i\pi/4)}{\sqrt{|\mathbf{r}-\mathbf{r}'|}} dl' \qquad (1)$$

where $\mathbf{r} = \{x, y\}$ is an arbitrary point, $\mathbf{r}' = \{x', y'\}$ is a point on the trajectory T where the complex EM field u is given, φ is the angle between the normal to T and $\mathbf{r} - \mathbf{r}'$, and dl' is the differential path along T.

[13] Processing of RO data is done in the following steps (geometry is shown in Figure 3).

1. The straight line GPS-LEO is defined for their median positions during a RO, as shown by direction X in Figure 3.

2. An equivalent PS normal to X is taken at a distance L from LEO and x is set to 0 at the PS. The vector of magnetic field is calculated at $x = 0$ and projected onto the PS, as shown by direction Z in Figure 3. Direction Y is normal to X and Z.

3. The BP plane is defined by directions X and Y, thus it is assumed to be normal to the direction of elongation of the irregularities as mapped on the PS, Z.

4. Since the EM field is assumed to be independent of Z, the trajectories of the GPS and LEO are projected onto the BP plane (T_1 and T_2 in Figure 3).

5. The EM field recorded in T_2 is not stationary due to movement of the GPS along T_1. Since BP has to be applied for a stationary EM field, instead of the true X, Y positions of the GPS and LEO the virtual positions X', Y' and the virtual phase path s' are calculated. The GPS is "fixed" to its median position, $x'_1 =$

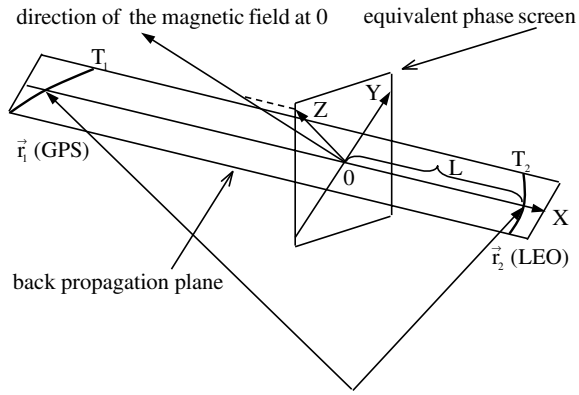

Figure 3. Geometry of the BP plane with account for the direction of the magnetic field. $\mathbf{r}_1$ and $\mathbf{r}_2$ originate at the center of the Earth.

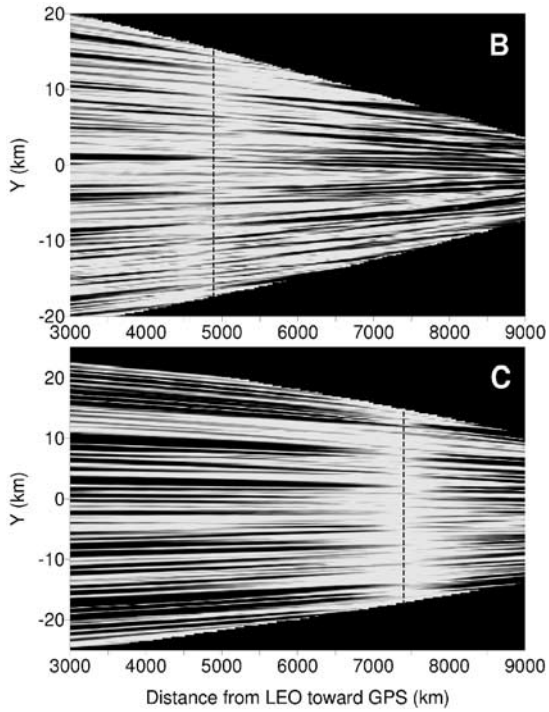

Figure 4. Amplitude modulation of the BP EM field for two GPS/MET occultations.

const, $y'_1 = 0$. The Y position of LEO at each time is corrected for the shift of the position of the GPS in the BP plane, $x'_2 = x_2$, $y'_2 = y_2 + y_1 x_2/x_1$. The virtual phase path is then $s' = \Delta s + s'_0$ where Δs is the true excess phase path measured in RO and $s'_0 = [(x'_2 - x'_1)^2 + (y'_2 - y'_1)^2]^{1/2}$ is the virtual phase path in vacuum. Thus the complex EM field $u' = a\exp(iks')$ is an approximation for the stationary EM field that would be observed along the virtual LEO trajectory T'_2 when the virtual GPS is "fixed" to median position.

6. BP is performed in the X, Y plane by using $u'(x', y')$ as the boundary condition. The position x^* of the minimum in rms of amplitude modulation in Y direction is estimated.

7. If $x^* \neq 0$ it means that the equivalent phase screen which models the irregularities must be located at different L. In this case the processing is repeated from step (2) for a different L (thus, for a different orientation of the BP plane). When x^* is close enough to zero (we used 100 km tolerance) then that L is used as an estimate of the distance from the LEO to the irregularities.

3. Analysis of GPS/MET Radio Occultation Data

[14] For RH processing we have selected 285 occultations (out of about 11,000 from the entire GPS/MET mission) characterized by S4>0.1 calculated between 40 and 80 km of TP altitude (as indicated by dashed lines in Figure 1). Next, we considered 35 occultations that resulted in a clear minimum of the BP amplitude modulation above the E layer. For automated processing, we characterized amplitude modulation by the RMS of $(a - \bar{a})/\bar{a}$ where $\bar{a}$ is the mean amplitude calculated in the Y direction. In most cases the irregularities were found at equatorial latitudes and at altitudes of several hundred kilometers. In some cases the irregularities were localized at very high altitudes above the F2 peak. Figure 4 shows two examples of the BP amplitude modulation for two occultations; the corresponding GPS/MET RO amplitudes are shown in Figures 1B and 1C. Figure 4B shows a minimum of the BP amplitude modulation at a distance $L \sim 4800$ km from LEO that corresponds to a rather commonly estimated altitude of the irregularities of about 300 km (occ. 481, Oct. 21, 1995, 17:41UTC, 2.5°S, 67°E). Figure 4C shows the minimum of amplitude modulation at $L \sim 7300$ km that corresponds to a very high altitude of the irregularities of about 1300 km (occ. 278, Mar. 20, 1996, 10:03UTC, 25.5°N, 155°W).

4. Discussion

[15] The results of the computational simulations and processing of the GPS/MET RO data indicate the possibility for detection and localization of the ionospheric irregularities at high altitudes above the F2. This can be potentially useful for transionospheric radio communications, as well as for study of the structure of the upper ionosphere.

[16] In order to be localizable the irregularities must occupy a volume whose dimension is less than the distance to the GPS and to the LEO. The effect of the irregularities on the wave propagation must be equivalent to the effect of the phase screen. In particular, that means that the amplitude modulation induced by the irregularities must be small inside the volume. For high-altitude irregularities a volume of about 10^3 km thickness along the LS can be fairly well localizable.

[17] The ranging error along the LS depends on error in the estimated direction of the irregularities. If we assume that the direction error is only related to the magnetic field mismodeling, then this error can be rather small, normally less than a few degrees. The 15° error, which results in 200–300 km ranging error, was used in the simulations for demonstration purposes.

[18] At present, validation of the results obtained in this study with the use of correlative data is rather difficult due to a lack of correlative data and due to rapid change of the ionospheric state. Evidence for electron density irregularities at high altitudes was provided by *Aarons et al.* [1996]. This paper presents a feasibility study. Validation must be addressed in the future. With the deployment of the COSMIC mission >2500 occultations per day will be available. This may provide sufficient data for validation of the technique and allow for the near real time monitoring of ionospheric irregularities.

[19] **Acknowledgments.** This research was supported by the Office of Naval Research, Award N00014-00-C-0291, and by the National Science Foundation through its support for the COSMIC data analysis and archive center (CDAAC) through grant number ATM-9732665 SP0-10.

References

Aarons, J., M. Mendillo, R. Yantosca, and E. Kudeki, GPS phase fluctuations in the equatorial region during the MISETA 1994 campaign, *J. Geophys. Res.*, *101*(A12), 26,851–26,862, 1996.

Barton, C. E., International geomagnetic reference field: the seventh generation, *J. Geomag. Geoelectr.*, *49*, 123–148, 1997.

Baker, B. B., and E. T. Copson, *The Mathematical Theory of Huygens' Principle*, Chelsea Pub. Co., N.Y., 193 pp., 1987.

Gorbunov, M. E., A. S. Gurvich, and A. V. Shmakov, Back-propagation and radio-holographic methods for investigation of sporadic ionospheric E-layers from Microlab-1 data,, *Int. J. Remote Sens.*, 2002 (in press).

Hajj, G. A., and L. J. Romans, Ionospheric electron density profiles obtained with the Global Positioning System: Results from the GPS/MET experiment, *Radio Sci.*, *33*(1), 175–190, 1998.

Hocke, K., and T. Tsuda, Gravity waves and ionospheric irregularities over tropical convection zones observed by GPS/MET radio occultation, *Geophys. Res. Lett.*, *28*(14), 2815–2818, 2001.

Kunitsyn, V. E., Determination of the structure of the nonuniformities of the ionosphere, *Geomagn. and Aeronomy*, *26*(1), 58–62, 1986.

Kursinski, E. R., G. A. Hajj, J. T. Schofield, R. P. Linfield, and K. R. Hardy, Observing Earth's atmosphere with radio occultation, *J. Geophys. Res.*, *102*(D19), 23,429–23,465, 1997.

Martin, J. M., Simulation of wave propagation in random media: theory and applications, in *Wave Propagation in Random Media (Scintillations)*,

edited by V. I. Tatarskii, A. Ishimaru, and V. U. Zavorotny, SPIE Press, Bellingham, WA, and the Institute of Physics Publishing, Bristol, UK, 463–486, 1993.

Rocken, C., et al., Analysis and validation of GPS/MET data in the lower troposphere, *J. Geophys. Res.*, *102*(D25), 29,849–29,866, 1997.

Schmidt, G., and A. Tauriainen, The localization of Ionospheric Irregularities by the Holographic Method, *J. Geophys. Res.*, *80*(31), 4313–4324, 1975.

Schreiner, W. S., S. V. Sokolovskiy, C. Rocken, and D. Hunt, Analysis and validation of GPS/MET radio occultation data in the ionosphere, *Radio Sci.*, *34*(4), 949–966, 1999.

Sokolovskiy, S. V., Inversions of radio occultation amplitude data, *Radio Sci.*, *35*(1), 97–105, 2000.

Tereshchenko, E. D., Determination of the height of ionospheric inhomogeneities by radio holography, *Geomagn. and Aeronomy*, *26*(4), 340–342, 1998.

Vorob'ev, V. V., A. S. Gurvich, V. Kan, S. V. Sokolovskiy, O. V. Fedorova, and A. V. Shmakov, Structure of the ionosphere based on radio occultation data from GPS "Microlab-1" satellites: Preliminary results, *Earth Obs. Rem. Sens.*, *15*, 609–622, 1999.

D. Hunt, C. Rocken, W. Schreiner, and S. Sokolovskiy, University Corporation for Atmospheric Research, Boulder, CO 80307-3000. (dhunt@ucar.edu; rocken@ucar.edu; schrein@ucar.edu; sergey@ucar.edu)